

Ripening of Porous Media

Benny Davidovitch, Deniz Ertaş and Thomas C. Halsey

Corporate Strategic Research, ExxonMobil Research and Engineering, 1545 Route 22 East, Annandale, NJ 08801

(Dated: October 22, 2002)

We address the surface tension-driven dynamics of porous media in nearly saturated pore-space solutions. We linearize this dynamics in the reaction-limited regime near its fixed points – surfaces of constant mean curvature (CMC surfaces). We prove that the only stable interface for this dynamics is the plane, and estimate the time scale for a CMC surface to become unstable. We also discuss the differences between open and closed system dynamics, pointing out the unlikelihood that CMC surfaces are ever realized in these systems on any time scale.

PACS numbers: 61.43.Gt, 47.70.-n, 47.54.+r

When solid grains are suspended in a solution saturated with the molecular constituents of the grains, they undergo coarsening under the thermodynamic driving force of surface tension. During this phenomenon, known as Ostwald ripening, the free energy of the system is lowered by minimizing the contact area between the coexisting phases. Molecules dissolve from high-curvature areas of the interface, pass through the solution, and can precipitate in low-curvature surface regions. This dynamics can be very complicated and depends on many parameters such as chemical composition, induced temperature and pressure fields, and other factors.

In this Letter we study Ostwald ripening in porous media, where the fluid in the pore space is approximately saturated with the ingredients of the solid phase. An example would be a sedimentary material such as sandstone, with the water in the pore space saturated with the silica components of the rock. Another example would be crushed ice, with water vapor saturating the air in the pore space between ice grains. We identify the fixed points of dissolution-precipitation dynamics as surfaces of “Constant Mean Curvature”, (CMC surfaces), and then show quite generally that these surfaces are unstable fixed points of this dynamics.

If one suspends grains in a solution, a mean field theory due to Lifshitz-Slyozov and Wagner is successful in capturing the dynamics at late stages of the ripening process for low solid volume fraction [1]. Another example of surface tension driven ripening arises in the kinetics of foams [2]. Unlike these examples, in typical porous media both the solid and pore space components of the medium are connected.

We thus pursue an approach more suited to porous media. Following [3] we consider the evolution of an interface $\Gamma(t) \equiv \mathbf{x}(u(t), v(t))$ between a porous, single component, isotropic solid and its ideal solution in the interstitial fluid. The solid is subject to a first order dissolution-precipitation reaction in a flow field of velocity \mathbf{v} . The normal velocity of the surface $u_n(\mathbf{x})$ into the pore space is given by

$$u_n(\mathbf{x}) = -K_f \left(1 - e^{-\frac{\Delta\mu(\mathbf{x})}{kT}} \right), \quad (1)$$

where K_f is the dissolution rate, and the precipitation rate is controlled by the Boltzmann factor associated with the difference $\Delta\mu(\mathbf{x}) \equiv \mu_{\text{sur}}(\mathbf{x}) - \mu_{\text{sol}}(\mathbf{x})$ between the chemical potentials of solid and dissolved molecules at the interface Γ . Referred to the chemical potential μ_{flat} for a flat surface in equilibrium with an ideal saturated solution of concentration c_{sat} , these are given by

$$\mu_{\text{sur}}(\mathbf{x}) = \mu_{\text{flat}} + 2\nu_m\sigma H(\mathbf{x}), \quad (2)$$

$$\mu_{\text{sol}}(\mathbf{x}) = \mu_{\text{flat}} + kT \log \frac{c(\mathbf{x})}{c_{\text{sat}}}, \quad (3)$$

where ν_m is the molecular volume in the solid, σ is the interfacial energy, $c(\mathbf{x})$ is the concentration near the surface point \mathbf{x} , and $H(\mathbf{x}) \equiv (1/2)(\delta S/\delta V)$ is the mean curvature, which measures the local variation in surface area δS with respect to a volume change δV of the solid. Here and elsewhere we define all concentrations with respect to the concentration in the solid. For $\Delta\mu \ll kT$, Eq. (1) reduces to

$$u_n(\mathbf{x}) = -K_f \frac{2\nu_m\sigma}{kT} \left[H(\mathbf{x}) - \frac{kT}{2\nu_m\sigma} \log \frac{c(\mathbf{x}, t)}{c_{\text{sat}}} \right]. \quad (4)$$

Since H should be no larger than the inverse of a typical pore size L , $H \sim L^{-1}$, and $\nu_m\sigma/kT$ is usually the inverse of a molecular scale,

$$\frac{\nu_m\sigma}{kT} \gg H, \quad (5)$$

we see that the linearized form of the dynamics holds for a nearly saturated solution $c \approx c_{\text{sat}}$.

The transport of the concentration field c in the solution is described by the advection-diffusion equation, with the appropriate boundary condition at the solid interface [3]. The velocity field satisfies the Navier-Stokes equation, with appropriate boundary conditions at infinity and at the solid surfaces inside the porous medium.

Since the full solution of these equations in a porous medium is daunting, we concentrate on two limiting cases of this problem, which we term “perfect open” and “perfect closed” systems. In a perfect open system, the velocity of the flow through the medium is considered sufficiently rapid that in effect each element of the surface

is in contact with fluid whose concentration c of the solute is fixed by a distant reservoir. This criterion can be achieved by taking the limit of small Damköhler number $Da \equiv K_f/v \rightarrow 0$, with v the average velocity of flow through the system [4]. Most of this study will concentrate on this limit. The other limit of a “perfect closed” system, in which $v = 0$ and the diffusion constant $D \rightarrow \infty$, will be explored at the end of this Letter.

In the perfect open case, the concentration $c(\mathbf{x})$ on the solution side of the interface has the constant value c_∞ , and the interface dynamics is governed only by Eq. (4), which yields

$$u_n(\mathbf{x}) = -K_f \frac{2\nu_m\sigma}{kT} [H(\mathbf{x}) - H_\star], \quad (6)$$

where $H_\star \equiv [kT/(2\nu_m\sigma)] \log(c_\infty/c_{\text{sat}})$.

CMC surfaces, for which $H(\mathbf{x}) = H_\star$ everywhere on the surface, are the fixed points of the dynamics (6). These surfaces have been studied in a variety of contexts, notably for their relationship to certain phases of block co-polymers [5]. The simplest examples are a sphere of radius $r = \frac{1}{2H}$ and a cylinder of radius $r = \frac{1}{2H}$.

A special case of CMC surfaces are “minimal surfaces”, for which $H(\mathbf{x}) = 0$. These surfaces have been extensively studied in the context of analytic function theory, and many such surfaces have been discovered [6]. For $H_\star = 0$, Eq. (6) is the equation of motion for a manifold seeking to minimize its own surface area, a dynamics that is sometimes called “motion under mean curvature” [7]. Of particular interest in the context of porous media are the triply periodic minimal surfaces, of which the Schwartz P-surface, shown in Fig. 1(a), is a classic example. Note that both sides of the surface form connected components, as in most porous media. Anderson *et al.* have extended several such surfaces into CMC surfaces with $H \neq 0$ [8]. The extension of the Schwartz P-surface to a family of CMC surfaces is shown in Fig. 2, with an example depicted in Fig. 1(b). These surfaces vary continuously from the P-surface (M) to a simple cubic lattice of barely touching spheres at one endpoint (A), and to a simple cubic lattice of barely touching spherical holes at the other endpoint (A') (see Fig. 2). Anderson *et al.* also generated families corresponding to fcc, bcc, and diamond lattices of spheres, with qualitatively similar properties. Although we are aware of no reported examples of “amorphous” families of CMC surfaces, it is likely that such families exist [9]. Such families would be most relevant to real porous media.

We now show that all CMC surfaces with the exception of planes are unstable fixed points of Eq.(6). Consider a surface $\mathbf{x}'(u, v) = \mathbf{x} + \epsilon(\mathbf{x})\mathbf{n}(\mathbf{x})$, whose deviation from a CMC surface $\mathbf{x}(u, v) \in \Gamma_\star$ with $H(\mathbf{x}) = H_\star$ is given by a (small) normal displacement $\epsilon(\mathbf{x})$. In [9] we show that the corresponding variation $\delta H(\mathbf{x}) = H(\mathbf{x}') - H_\star$ is given

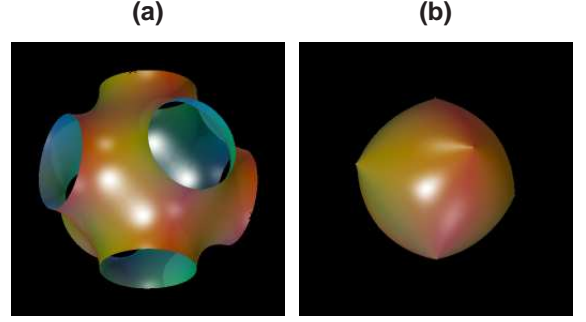


FIG. 1: (a) The Schwartz P-surface, a minimal (zero mean curvature) surface of simple cubic symmetry. A single unit cell is shown. (b) A single unit cell of size L of a CMC surface with $HL \approx 2.0$, which is close to a simple cubic lattice of touching spheres. Figures courtesy of J.T. Hoffman, MSRI Scientific Graphics Project, UC Berkeley [10].

to first order in ϵ by

$$\delta H(\mathbf{x}) = - \left[(2H_\star^2 - K)\epsilon + \nabla_s B \cdot \nabla_s \epsilon + \frac{1}{2} \nabla_s^2 \epsilon \right], \quad (7)$$

$$B(\mathbf{x}) \equiv -\frac{1}{8} \log(H_\star^2 - K(\mathbf{x})), \quad (8)$$

where ∇_s and ∇_s^2 are the surface gradient and Laplacian, respectively, and $K(\mathbf{x})$ is the Gaussian curvature at \mathbf{x} . Substituting Eq. (7) in (6), we obtain the linear dynamics near a CMC surface with mean curvature H_\star

$$\frac{\partial \epsilon}{\partial t} = \frac{2K_f\nu_m\sigma}{kT} \mathcal{L}\epsilon, \quad (9)$$

$$\mathcal{L} \equiv 2H_\star^2 - K + \nabla_s B \cdot \nabla_s + \frac{1}{2} \nabla_s^2. \quad (10)$$

Recall the definition of H and K in terms of the local principal radii of curvature of the surface R_1 and R_2 ,

$$H = (R_1^{-1} + R_2^{-1})/2, \quad ; \quad K = (R_1 R_2)^{-1}.$$

Since $2H^2 - K = (R_1^{-2} + R_2^{-2})/2 \geq 0$, uniform precipitation ($\epsilon > 0$) decreases the curvature, making the surface locally more hospitable to deposition, while dissolution ($\epsilon < 0$) increases the curvature, favoring further dissolution. This observation already suggests that the surface is likely to be unstable.

Because the term in \mathcal{L} which couples Gaussian curvature gradients with the gradient of ϵ is non-Hermitian, it is more convenient to work with the Hermitian operator \mathcal{H} defined via the “gauge transformation”

$$\mathcal{H} \equiv e^{B(\mathbf{x})} \mathcal{L} e^{-B(\mathbf{x})} \quad (11)$$

so that

$$\mathcal{H} = V(\mathbf{x}) + \frac{1}{2} \nabla_s^2, \quad (12)$$

$$V(\mathbf{x}) = 2H_\star^2 - K - \frac{1}{2} [\nabla_s^2 B + (\nabla_s B)^2]. \quad (13)$$

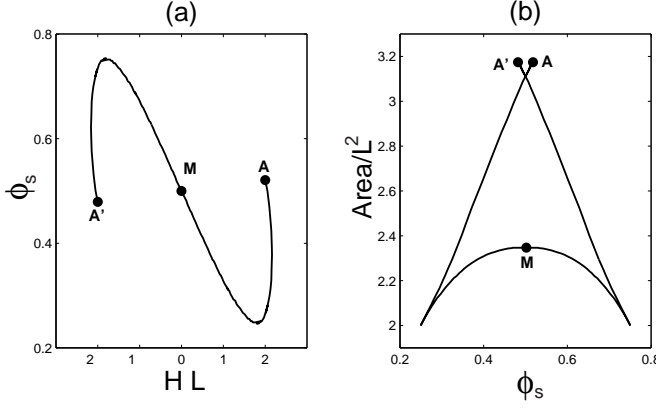


FIG. 2: (a) The curvature HL versus volume fraction ϕ_s for the constant mean curvature extension of the Schwartz P-surface with unit cell size L . The minimal ($H=0$) P-surface is represented by the point M , and the endpoints correspond to (A) a simple cubic lattice of touching spheres, and (A') a simple cubic lattice of touching spherical holes. (b) The surface area $/L^2$ per unit cell of size L versus enclosed solid volume fraction ϕ_s for the same simple-cubic CMC family. The lower branch is stable under periodic, volume-preserving, surface-minimizing dynamics. Figure adapted from Ref. [8], courtesy of Advances in Chemical Physics.

The eigenvalues of \mathcal{H} are identical to those of \mathcal{L} [11], and they are bounded from above provided that $V(\mathbf{x}) < \infty$.

For any function $\Psi(\mathbf{x})$ defined on the surface, a lower bound on the maximum eigenvalue ω_0 of \mathcal{H} (consequently \mathcal{L}) can be established using the inequality

$$\omega_0 \geq \frac{\int_{\Gamma} dS \bar{\Psi}(\mathcal{H}\Psi)}{\int_{\Gamma} dS |\Psi|^2}, \quad (14)$$

where $\int_{\Gamma} dS$ is the ordinary surface integral. Using the trial function $\Psi_B(\mathbf{x}) = e^{B(\mathbf{x})}$, we obtain

$$\begin{aligned} \omega_0 &\geq \frac{\int_{\Gamma} dS (H_{\star}^2 - K)^{-1/4} (2H_{\star}^2 - K)}{\int_{\Gamma} dS (H_{\star}^2 - K)^{-1/4}} \\ &= H_{\star}^2 + \frac{\int_{\Gamma} dS (H_{\star}^2 - K)^{3/4}}{\int_{\Gamma} dS (H_{\star}^2 - K)^{-1/4}}. \end{aligned} \quad (15)$$

However, since $H^2 - K = [(1/R_1) - (1/R_2)]^2/4$ is non-negative everywhere on the surface and reaches zero homogeneously on Γ only for a planar surface, we conclude that *the only marginally stable fixed point of the dynamics (6) is the plane*. There are no other surfaces of any kind, porous or non-porous, that are metastable under Ostwald ripening. This conclusion applies both to periodic and to possible amorphous CMC surfaces. For a system with a pore scale of L , we expect this instability to manifest itself on a time scale of

$$\tau_{\text{ripen}} = \frac{kTL^2}{K_f \sigma \nu_m}. \quad (16)$$

Note that intuitively, the instability is enhanced by an increase in the magnitude either of the mean curvature, or of the Gaussian curvature (since the latter is on average negative for a surface of large genus, such as a typical porous surface.)

For triply periodic CMC surfaces, the periodicity of the “potential” $V(\mathbf{x})$ implies that the eigenmodes $\Psi_{\mathbf{k},n}(\mathbf{x})$ of the operator \mathcal{H} (and of \mathcal{L}) are surface Bloch functions,

$$\mathcal{H}\Psi_{\mathbf{k},n}(\mathbf{x}) = \omega_{\mathbf{k},n} e^{i\mathbf{k}\cdot\mathbf{x}} U_{\mathbf{k},n}(\mathbf{x}) \quad (17)$$

$$U_{\mathbf{k},n}(\mathbf{x}) = U_{\mathbf{k},n}(\mathbf{x} + \mathbf{R}) \quad (18)$$

where \mathbf{R} is a lattice vector, \mathbf{k} is the crystal momentum (confined to the first Brillouin zone), and n is a discrete label distinguishing between different branches. Standard techniques should allow determination of the spectrum of \mathcal{H} throughout the first Brillouin zone [9].

As a concrete example, we have computed the positive eigenvalue ω_0 corresponding to the $\mathbf{k} = \mathbf{0}$ eigenmode $\Psi_0(\mathbf{x}) \equiv U_{0,0}(\mathbf{x})$ for the Schwartz P-surface numerically by maximizing the functional on the RHS of Eq. (14). The details of the maximization procedure will be presented elsewhere [9]. We obtain $\omega_0 \approx 6.1$ for a unit cell of size $L = 1$, whereas the lower bound implied by Eq. (15) is $\omega_0 \geq 2.9$.

Since the eigenfunction of the largest eigenvalue has the same sign (precipitation or dissolution) everywhere on the surface, the unstable dynamics of Eq. (6) involves transport of solute into (or out of) the pore space from the distant reservoir. Therefore, the nature of the dynamics might be different in a closed system, where the total amount of the solid component is conserved.

In a “perfect closed” system, we further regard the surface motion as reaction limited, such that the solute concentrations near the entire surface are approximately equal to the average concentration in the pore \bar{c} . This condition is satisfied at the pore scale L if $D \gg K_f L / c_{\text{sat}}$. By integrating Eq. (4), we see that \bar{c} must then approach a value c_{eq} determined by

$$\log \frac{c_{\text{eq}}(\bar{H})}{c_{\text{sat}}} = \frac{2\nu_m \sigma \bar{H}}{kT}, \quad (19)$$

controlled by the average mean curvature \bar{H} of the surface, over a characteristic time scale $\tau_{\text{pore}} = Lc_{\text{sat}}/K_f$. For $\tau > \tau_{\text{pore}}$, the solute concentration \bar{c} is “slaved” to $c_{\text{eq}}(\bar{H})$. Conservation of the total solid requires

$$\phi_t = \phi_s + \bar{c}(1 - \phi_s), \quad (20)$$

where ϕ_s is the solid volume fraction enclosed by the surface and ϕ_t would be the solid volume fraction if none of the solid were dissolved. Eliminating $\bar{c} = c_{\text{eq}}(\bar{H})$ from Eq. (20) using Eq. (19) shows that ϕ_s is very insensitive to the value of \bar{H} ,

$$\left| \frac{d \log \phi_s}{d \log \bar{H}} \right| \approx \frac{2c_{\text{sat}}(1 - \phi_t)}{\phi_s(1 - c_{\text{sat}})^2} \frac{\nu_m \sigma |\bar{H}|}{kT} \ll 1, \quad (21)$$

where we have used Eq. (5). In a “perfect closed” system, we take ϕ_s constant, which is an excellent approximation for $\tau > \tau_{\text{pore}}$. This dynamics is now given by Eq. (6) with the constant H_\star replaced by \bar{H} , whose evolution with time is controlled by the constraint of constant $\phi_s \approx (\phi_t - c_{\text{sat}})/(1 - c_{\text{sat}})$. This is surface area minimization under the constraint that the volume contained within the surface is conserved.

Consider again periodic surfaces of the Anderson type. Figure 2(b) shows the total surface area as a function of ϕ_s along the manifold of CMC surfaces of simple cubic structure. Although all CMC solutions represent fixed points of the dynamics, we anticipate that for a given ϕ_s , only the CMC surface with the lowest area can be stable under these dynamics, and only if the system is also required to maintain its spatial periodicity. We have confirmed this by direct simulation using Surface Evolver [9, 12]. This result is an extension of the well-known stability of the minimal surface (point M in Fig. 2) to the entire lower branch in Fig. 2(b), under periodic surface area minimization dynamics with conserved volume. A corollary of this result is that along this lower branch, \mathcal{L} has only one unstable $\mathbf{k} = \mathbf{0}$ mode [9], which is disallowed by solid conservation under closed system dynamics. Thus the stable mode with the longest relaxation time τ_{relax} will control approach to the stable CMC surface; dimensional analysis suggests that $\tau_{\text{relax}} \sim \tau_{\text{ripen}}$.

Nevertheless, for an extended system this apparent stability is compromised by the unstable hydrodynamic ($\mathbf{k} \neq 0$) modes in the eigenvalue spectrum Eq. (17), which do conserve the overall ϕ_s . It is possible for these unstable modes to be restricted to the topmost ($n = 0$) band and to wavevectors $k < \pi/\ell_0$, such that transport of solute over length scales $> \ell_0$ is needed to activate these modes. For amorphous surfaces, the band structure picture is not appropriate, but we still expect unstable modes to appear above a characteristic length scale $\ell_0 \gtrsim L$. In either case, it is natural to ask if there is a window of time over which the CMC surfaces might be observable, before the instability manifests itself.

During the time τ_{relax} characterizing the relaxation to the CMC surface, the diffusion length over which solid transport is possible is $\ell_D = \sqrt{D\tau_{\text{relax}}}$. Using the reaction-limited constraint $D \gg K_f L/c_{\text{sat}}$ and $\tau_{\text{relax}} \sim \tau_{\text{ripen}}$, with τ_{ripen} given by Eq. (16), we find

$$\frac{\ell_D}{L} \gg \sqrt{\frac{kTL}{\sigma\nu_m c_{\text{sat}}}} \gg 1 \quad (22)$$

where the last inequality follows from Eq. (5). Since we thus expect $\ell_D \gg \ell_0$, by the time a surface relaxes on the pore scale to a CMC surface, the diffusive transport between pores will have activated the unstable dynamics, taking the system away from this surface. Thus we do not expect an intermediate-time window over which CMC

surfaces would be seen [13].

Using representative values for K_f and σ for quartz in water [14], we get for $L \sim 100 \mu\text{m}$ that $\tau_{\text{ripen}} \sim 500$ million years, a time scale over which geological systems should be regarded as open. However, a similar estimate for limestone yields a value of $\tau_{\text{ripen}} \sim 7$ years, which is quite short on geological time scales, so that these systems will correspond more closely to closed systems [15]. Of course for real geological systems these processes involve complicated multicomponent equilibria, and other mechanisms such as pressure solution may dominate as well [16]. Nevertheless, there are probably geological circumstances under which surface-tension driven phenomena will be important.

We would like to thank I. Androulakis, P. Chaikin, S. Milner, and T. Witten for helpful and informative discussions. A. Herhold and R. Polizzotti advised us on the properties of real sedimentary materials. K. Brakke assisted us with questions regarding the use of the Surface Evolver software. We are grateful to F. Leyvraz for pointing out an error in our reasoning, and to M. Hastings for bringing to our attention the “gauge” transformation used in Ref. [11].

-
- [1] I. Lifshitz and V. Slyozov, J. Phys. Chem. Solids **19**, 35 (1961); C. Wagner, Z. Electrochem. **65**, 581 (1961); P. W. Voorhees, Ann. Rev. Mats. Sci. **22**, 197 (1992).
 - [2] D. Weaire and S. Hutzler, *The Physics of Foams* (Oxford University Press, Oxford, 1999).
 - [3] S. Békri, J. Thovert, and P. Adler, Chem. Eng. Sci. **50**, 2765 (1995).
 - [4] G. Daccord, O. Liétard, and R. Lenormand, Chem. Eng. Sci. **48**, 179 (1993).
 - [5] E. Thomas, D. Alward, D. Kinning, D. Martin, J. Handlin, and L. Fetters, Macromolecules **19**, 2197 (1986).
 - [6] J. C. Nitsche, *Lectures on Minimal Surfaces* (Cambridge University Press, London, 1999).
 - [7] J. Sethian, *Level Set Methods and Fast Marching Methods* (Cambridge University Press, London, 1999), 2nd ed.
 - [8] D. Anderson, H. Davis, L. Scriven, and J. C. Nitsche, Adv. Chem. Phys. **77**, 337 (1990).
 - [9] B. Davidovitch, D. Ertaş, and T. C. Halsey, unpublished.
 - [10] <http://www.msri.org/publications/sgp/SGP/>.
 - [11] N. Hatano and D. R. Nelson, Phys. Rev. Lett. **77**, 570 (1996).
 - [12] <http://www.susqu.edu/facstaff/b/brakke/evolver>.
 - [13] This is only the case for connected pore spaces. Disconnected pore spaces, e.g., isolated spherical “vugs”, can obviously be stable.
 - [14] P. Dove, Am. J. Sci. **294**, 665 (1994); R. Iler, *The Chemistry of Silica* (John Wiley and Sons, New York, 1979).
 - [15] L. Plummer, T. Wigley, and D. Parkhurst, Am. J. Sci. **278**, 179 (1978); J. Mullin, *Crystallization* (Butterworth-Heinemann, Oxford, 2001), 4th ed.
 - [16] R. de Boer, Geochim. Cosmochim. Acta **41**, 249 (1977).